UCRL-JC-130117
PREPRINT

Magnetic Domain Structure and Magnetization Reversal in Submicron-Scale Co Dots

A. Fernandez
M. R. Gibbons
M. A. Wall
C. J. Cerjan

This paper was prepared for and presented at the
7th Magnetism and Magnetic Materials Intermag Conference
San Francisco, California
January 6-9, 1998

February 17, 1998

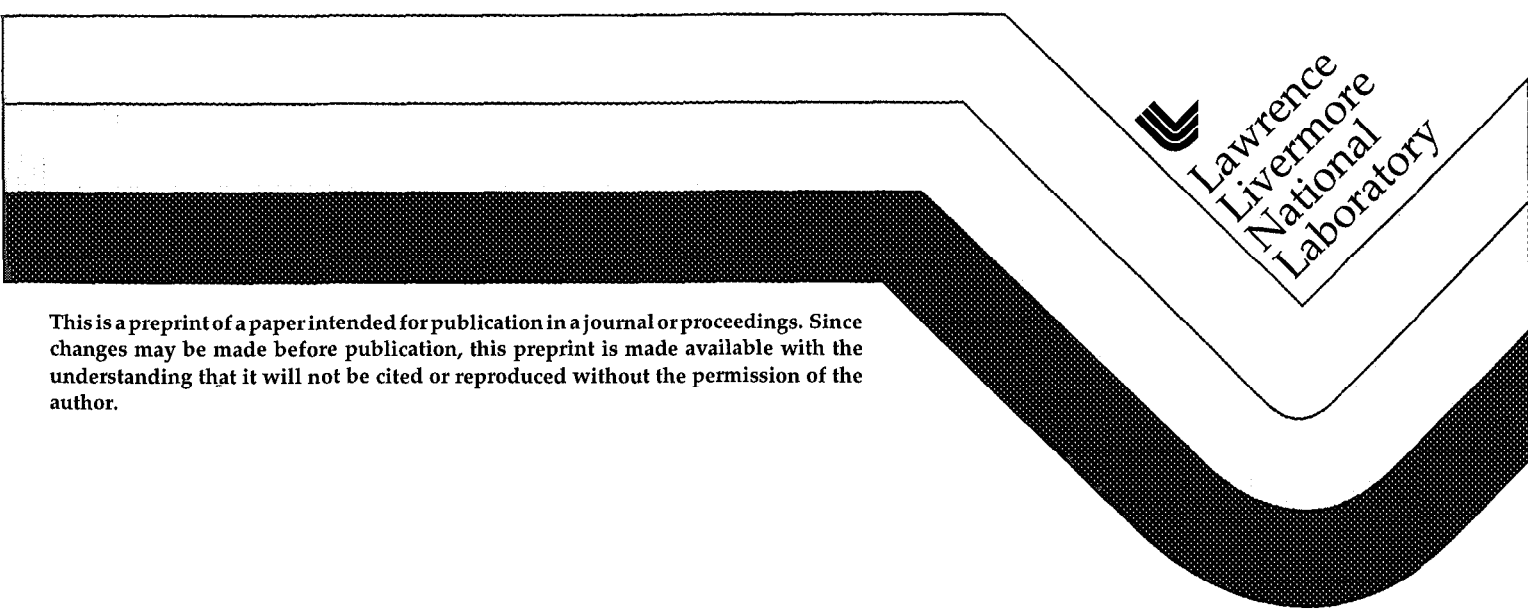

Magnetic domain structure and magnetization reversal in submicron-scale Co dots

A. Fernandez, M. R. Gibbons, M. A. Wall, and C. J. Cerjan

Lawrence Livermore National Laboratory, Livermore CA 94551

Abstract

We present a magnetic force microscopy (MFM) analysis of arrays of submicron-scale Co dots fabricated by interference lithography. The dots are thin (180-300 Å) and are elliptical in shape. MFM of these structures reveals that they relax into highly ordered remanent states whose symmetry and configuration are governed by their shape anisotropy. In particular, when the dots are saturated along the easy-axis, a uniformly magnetized state persists at remanence. However, when the dots are saturated in hard-axis, they relax into a single-vortex state in which the circulation can have either sign. Both remanent states are characterized by smoothly varying magnetization patterns and a high degree of uniformity across the array. We attribute the ordered behavior of these structures to the film microstructure, which allows the shape anisotropy to dominate over magnetocrystalline anisotropy. By imaging a series of minor-loop remanent states, we show that magnetization reversal in these structures occurs via the nucleation and annihilation of a single vortex. Magnetic hysteresis loop measurements are consistent with these observations and provide additional details. Furthermore, we present the results of micromagnetic simulations, which are in excellent agreement with both the MFM images and the hysteresis loop measurements.

Keywords:

Magnetic force microscopy, Co dots, remanent states, magnetization reversal, micromagnetic simulations.

Contact author:

Andres Fernandez
Lawrence Livermore National Laboratory
P.O. Box 808, L-395
Livermore, CA 94551

FAX: 510-422-8761
email: fernandez10@llnl.gov

1. Introduction

Recent interest in the magnetic properties of small, lithographically patterned magnetic structures has been motivated, in part, by the need to better understand the ultimate limits of magnetic recording densities. In addition, the domain patterns and reversal mechanisms of small magnetic structures play an important role in the operation of magnetoresistive and giant-magnetoresistive sensors, particularly as the size of these devices is pushed into the submicron regime where demagnetization effects are strong. The study of small magnetic structures also provides an excellent opportunity for testing micromagnetic simulations. These simulations, which can be used to model complex arrangements of magnetic materials, are computationally intensive and therefore are easier to test against structures that are small in size, relatively simple in shape, and have well characterized composition.

The correlation of the magnetic properties of patterned structures to the size and shape of the structures is a central issue that has been addressed in many recent studies [1-6]. It is well known that, in the limit of large geometries, magnetic materials generally display complicated multi-domain patterns. As the structure size is reduced, most materials possess simpler domain structures [7]. Eventually, the single-domain state is reached when exchange energy dominates over all other energetic contributions. Reversal in single-domain particles is classically described by the Stoner-Wolfarth (SW) model, which treats the reversal process as a coherent rotation of the magnetization [8]. In certain cases, such as that of small (~50 nm), low-aspect ratio structures, the SW model seems to agree rather well with the

1. Introduction

Recent interest in the magnetic properties of small, lithographically patterned magnetic structures has been motivated, in part, by the need to better understand the ultimate limits of magnetic recording densities. In addition, the domain patterns and reversal mechanisms of small magnetic structures play an important role in the operation of magnetoresistive and giant-magnetoresistive sensors, particularly as the size of these devices is pushed into the submicron regime where demagnetization effects are strong. The study of small magnetic structures also provides an excellent opportunity for testing micromagnetic simulations. These simulations, which can be used to model complex arrangements of magnetic materials, are computationally intensive and therefore are easier to test against structures that are small in size, relatively simple in shape, and have well characterized composition.

The correlation of the magnetic properties of patterned structures to the size and shape of the structures is a central issue that has been addressed in many recent studies [1-6]. It is well known that, in the limit of large geometries, magnetic materials generally display complicated multi-domain patterns. As the structure size is reduced, most materials possess simpler domain structures [7]. Eventually, the single-domain state is reached when exchange energy dominates over all other energetic contributions. Reversal in single-domain particles is classically described by the Stoner-Wolfarth (SW) model, which treats the reversal process as a coherent rotation of the magnetization [8]. In certain cases, such as that of small (~50 nm), low-aspect ratio structures, the SW model seems to agree rather well with the

experimental data [9]. But in other types of structures, the SW model is not followed, and more complex reversal mechanisms are required to describe the hysteresis behavior [2,10,11].

In the following, we describe experiments on polycrystalline Co structures whose magnetic properties fall into an intermediate regime between single-domain and multi-domain behavior. The structures are thin (180-300 Å), submicron in size, and are patterned with a well-defined in-plane shape anisotropy axis. The saturation remanent states of the dots are analyzed by magnetic force microscopy (MFM). These measurements show that well-ordered remanent states are formed which are strongly dictated by the size and shape of the dots. We contrast our measurements with previously reported MFM studies of similar Co particles [12], and we relate the differences in the observed magnetic behavior to differences in the microstructure of the Co. In addition, we perform micromagnetic simulations to model the magnetic response of the dots and compare the results to our MFM images. To gain insight into the reversal mechanism of the structures, we use MFM to image minor-loop remanent states. These measurements demonstrate that reversal in these Co structures occurs by the nucleation and annihilation of a single vortex.

2. Sample fabrication

Arrays of magnetic dots are produced by interference lithography and a lift-off process [13]. Interference lithography is a robust patterning technique that allows the fabrication of arrays of sub-quarter micron size structures using optical illumination and ordinary i-line resist processing. To achieve good lift-off profiles, a tri-layer

process is used. Silicon wafers are coated with 200 nm of polymethylmethacrylate (PMMA), 20 nm of plasma deposited SiO_2, an anti-reflective coating (ARC) and a layer of resist, in that order. The resist is exposed to an interference pattern formed at the intersection of two mutually coherent beams of 351.1 nm illumination. The period is controlled by adjusting the intersection angle and is fixed to 1μm for this study. After the first exposure, the sample is rotated 90° in the exposure plane and exposed a second time. Development after this step would normally produce a two-dimensional array of resist dots [14]. Instead, the samples are treated to an image reversal step that produces an array of resist holes upon development. Details of the image reversal process are reported elsewhere [15]. The aspect-ratio of the holes is controlled by varying the relative doses of the two orthogonal exposures. After development, reactive ion etching is used to transfer the hole pattern through the ARC, SiO_2 and PMMA layers. The etch is followed by thermal evaporation of a thin layer of Co (180-300 Å thick). The Co is capped with 50-80 Å of Au on some samples to prevent oxidation. Lift-off is performed in a solution of methylene chloride, which dissolves the PMMA layer.

A scanning electron micrograph of the completed structures is shown in Fig. 1. The dots are elliptical in shape with an aspect ratio of 1.6-1.8. They have sharply defined edges and are highly symmetric about their long- and short-axes. We estimate the edge roughness to be less than 8 nm. The size of the dots can be varied by adjusting the total exposure dose. In this paper, we only present results on dots that are nominally 450 nm × 250 nm in size.

Transmission electron microscopy shows that the Co films consist of hcp grains with an average grain size of 60 Å. Diffraction measurements indicate that the c-axes of the grains are randomly oriented in all directions. These films exhibit low coercivity values (~12 Oe), which can be directly attributed to the film microstructure. The relationship between the microstructure and the magnetic properties of the patterned structures will be addressed in more detail below.

Magnetic force microscopy is carried out using a Nanoscope Dimension 5000. All the images presented are phase images acquired using the LiftMode technique [16]. The MFM probe is magnetized perpendicular to the plane of the substrate. Prior to imaging the saturation remanent states of the arrays, the samples are placed in a uniform in-plane field of 4 kOe, which is subsequently ramped to zero. In Sec. 4, a more complicated magnetizing procedure is described.

3. Saturation remanent states

Magnetic force microscopy reveals that the Co dots relax into highly ordered remanent states whose symmetry is uniquely determined by the shape anisotropy of the structures. When 180 Å thick dots are saturated along their long-axis, a uniformly magnetized state persists at remanence, as shown by the image in Fig. 2(a). In this remanent state, the MFM images display a purely dipole character in which no other contrast is observed. Varying the tip-sample separation does not change the observed pattern but only results in a change in the signal amplitude. The absence of fine scale structure in the domain pattern implies that the local magnetization of the dots is highly uniform on a length scale comparable to the

MFM resolution (~20 nm). The image in Fig. 2(a) also indicates that the average magnetization of the dots is closely aligned with their long-axes. Thus, the easy-axis of magnetization is defined by the shape anisotropy. Furthermore, the large area image in Fig. 2(b) shows that the response of the dots is remarkably uniform across the array. This result is important from a technological perspective. It demonstrates that a uniform remanent state can be generated in a large collection of patterned structures despite the inherent variability associated with the polycrystalline make-up of the structures and the microfabrication process.

Although the easy-axis remanent state is a uniformly magnetized domain, the dots are not in a classical single-domain state, which would only be true if the this configuration were the only stable magnetic state. When the dots in Fig. 2 are saturated along the short-axis, they relax into an entirely different remanent state, which has the distinct MFM signature shown in Fig. 3. In this state, the images of the dots are divided into four equal quadrants that have alternating dark and light contrast. We interpret this contrast to indicate that the dots have formed a flux closure pattern in which a single magnetic vortex occupies the center of the dot. Both signs of circulation are represented in the array with equal probability. Because the single-vortex state is centered about both axes, zero net magnetization is expected. This is confirmed by magnetic hysteresis measurements, which are described in Sec. 5. The uniformity in response across the array is not as high as it is in the easy-axis state. We find that in this case 90% of the dots relax into the single-vortex pattern while 10% remain in a uniformly magnetized state.

We have examined the behavior of thicker Co dots (300 Å) and observe that their saturation remanent states are very similar to the ones described above except for two main differences. (1) In the easy-axis remanent state, the thicker dots cannot readily be imaged without the MFM tip disturbing the magnetic configuration. As the tip passes over some of these dots, they initially appear similar to the dots in Fig. 2, but then, quite suddenly, they irreversibly switch into a single-vortex state. As hysteresis loops show (see Sec. 5), the onset of magnetization reversal is close to zero field in thicker Co dots, which makes is easy for the MFM to perturb the easy-axis remanent state. (2) In the hard-axis state, the response uniformity across the array is actually improved over the thinner dots. We find that in this case 97% of the dots relax into the single-vortex state. Interestingly, the other 3% do not form a uniformly magnetized domain but instead support a double-vortex closure pattern. Both these differences can be qualitatively explained by the larger demagnetization field that is produced in thicker Co dots, as will be discussed in more detail in Sec. 5.

To better interpret the MFM data, we simulated the magnetic response of the dots with a micromagnetic model [17]. The algorithm advances the magnetization using the Landau-Lifshitz-Gilbert dynamic equation in a semi-implicit formulation. The magnetostatic potential is solved using finite difference on a Cartesian, nonuniform mesh. Included in the simulation is the elliptical shape of the dots, exchange coupling ($A=1.6\times10^{-6}$ erg/cm^2), and uniaxial crystalline anisotropy ($K_1=1.0\times10^{6}$ erg/cm^3). The crystalline axes are randomly oriented from grain to grain, and the mesh discretization is set the same as the grain size. The evolution of the magnetization pattern over a full hysteresis loop is calculated using 50 Oe steps.

Simulated MFM images are generated by assuming the tip interacts with the sample as a fixed point dipole, which is a reasonable first approximation [18]. The image is rendered from a gray scale contour plot of the quantity $-d^2H_z/dz^2$, calculated approximately 100 Å above the simulated dot.

While the size and grain structure of the simulated dots were based on measurement, the exchange and anisotropy constants were not known precisely. Bulk values were used and then varied slightly until a match with the measured hysteresis loop and MFM data was found. A simulated MFM image of the hard-axis remanent state is displayed in Fig. 4(a). Comparison of the simulation to the data in Fig. 2 shows a remarkably close match. As can be seen in Fig. 4(b), the simulation reveals that the source of the contrast in the MFM image is a single vortex with moments at the center forming a Néel-type core, as opposed to a Bloch-type core. Furthermore, the simulation shows that the direction of magnetization varies in a smooth and continuous fashion about the core. This behavior is in contrast to the four sharply defined domain walls typically calculated [19] and observed [7] in rectangular particles. The smooth magnetization variation is the cause of the somewhat atypical four-quadrant MFM image. The simulation results, which will be reported in more detail elsewhere [20], are also in good agreement with the easy-axis remanent state and in excellent quantitative agreement with the hysteresis loop measurements shown in Sec. 5.

The high degree of local uniformity exhibited by our Co structures is contrary to an earlier study by New *et al.* of similarly sized (400 nm × 200 nm) Co particles [12]. Unlike our observations, they found that the magnetic configuration of the

easy-axis remanent state contained a great deal of local disorder. Although MFM images of the hard-axis state were not reported, hysteresis loop measurements in the hard-axis direction indicated a large net remanence. This result is inconsistent with the formation of a uniform single-vortex state as we observe.

At first glance, the disparity in magnetic behavior between Co structures so closely matched in size and shape is surprising. However, the differences can be understood by considering the differences in the Co microstructure. In New's study, the Co was deposited by dc magnetron sputtering onto a Cr underlayer [12]. As a result, their films consisted of 100-200 Å size hcp grains that were highly textured with the c-axis in-plane. By contrast, our films are made using thermal evaporation, which is a less energetic deposition process than sputtering. Thermal evaporation yields films that have smaller grains (~60 Å) and are not textured. The combination of smaller grains and the lack of texturing size alters the relative balance between exchange and crystalline anisotropy energy. In the limit that grain sizes are large compared to typical domain wall widths, crystalline anisotropy will force the domains to align with the easy-axis of the crystallites, thereby causing local disorder in the direction of the magnetization. As grain sizes decrease, exchange energy rises in proportion to the domain wall density, which initially scales as the inverse square of the grain size. In the limit that grain sizes are small compared to domain wall widths, the intergrannular exchange coupling will dominate and will smooth out the effects of crystalline anisotropy. The domain wall width is approximately given by $\pi\sqrt{A/K_1}$, which yields a typical wall width of 190 Å in Co. The lack of in-plane texturing further reduces the contribution of crystalline anisotropy to the

energy. Thus we can expect our Co films to have comparatively stronger intergrannular exchange coupling, which is evident by the much lower coercivity of our films (~12 Oe) compared to the sputtered films in New's study (~350 Oe). Under these conditions, the disordered domain configurations of the sputtered structures will be replaced by configurations that are dictated by the in-plane demagnetization field.

4. Magnetization reversal

A common approach to study reversal processes using MFM is to measure a series of minor-loop remanent states [21]. The structures are first saturated in an applied field. The field is then reduced to a fixed negative value H_m, after which it is ramped to zero. The remanent state is then imaged in the MFM. This sequence is repeated multiple times, and each time the value of H_m is incremented. In cases where reversal occurs over a narrow field range, this procedure has been effective for determining the approximate switching field of the structures [2,11]. In addition, it may be possible to capture the structure in a stable intermediate configuration, which can provide valuable clues to the reversal mechanism.

We have applied the minor-loop approach to determine the reversal mechanism in the 300 Å thick Co dots in the easy-axis. We find that for fields in the range of 0 Oe to -200 Oe, the minor loop remanent states consist of a mixture of dots that are uniformly magnetized and dots that contain a single-vortex. In this range, the number of dots that have not nucleated a vortex decreases rapidly with increasing negative field. Below a field of -300 Oe, almost all of the dots have

nucleated into a single-vortex state (Fig. 5). (A small percentage of the dots, ~3%, nucleate a double-vortex closure pattern, which are not shown in the figure.) Increasing the field to greater negative values has no effect until a second threshold is reached at ~-900 Oe. At this point the vortex pattern begins to disappear in some dots. Below a field of -1 kOe, all the dots have completely reversed to a uniformly magnetized state of opposite sign.

We can infer from the above observations that magnetic reversal in these structures occurs predominantly by the nucleation and annihilation of a single magnetic vortex. This well-ordered reversal process contrasts with the more varied reversal mechanisms observed for the sputtered Co structures discussed earlier [22]. The fact that in some ranges of field the minor-loop remanent states are composed of a mixture of domain states implies that field values for vortex nucleation and annihilation vary to some degree across the array. Such variation may have several sources. Size variation, edge roughness, and the polycrystalline make-up of the dots may all contribute to a complicated energy surface that gives rise to a distribution of nucleation and annihilation fields. By sampling a large number of dots in a mixed minor-loop state, we may be able to correlate the magnetization pattern to variations in size as measured in the topographic part of the scan. Determining the relative contribution of edge roughness and other factors may be more difficult. It is important to emphasize that despite the variability in nucleation fields caused by different dot morphologies, approximately 97% the dots in our arrays reverse their magnetization by the same exact mechanism.

5. Magnetic hysteresis loops

Magnetic hysteresis loops of the patterned structures provide a complementary picture to the MFM analysis given above. In Fig. 6(a) and 6(b) are the measured loops in the easy-axis direction and in the hard-axis direction, respectively, for an array of 300 Å thick dots. The easy-axis loop shows a large remanence and a coercivity of 155 Oe, which is more than 10 times greater than the sheet film coercivity. In contrast, the hard-axis loop shows zero remanent magnetization. Moreover, the hysteresis loop is closed over a central portion of the loop. These results are consistent with the interpretation of the MFM data that a single magnetic vortex occupies the center of the dots at remanence. The closure of the loop near zero field is in an indication that the vortices can move freely within the dots without being impeded by defects or other dissipative effects.

The hysteresis loops in Fig. 6 are very similar in shape to the ones measured by Wernsdorfer *et al.* for a single Co particle using a highly sensitive SQUID technique [23]. Their Co structures measured 300 nm × 200 nm in size and were also produced by thermal evaporation. As their data and our data shows, the easy-axis and hard-axis loops are characterized by two relatively abrupt changes in magnetization, which are marked by the symbols H_n and H_a in both graphs. From our MFM analysis, the significance of these transitions is clear. The first transition H_n marks the nucleation of a vortex at one edge of the dot, while the second transition H_a marks the annihilation of the vortex at the opposite edge. The shift of the measured nucleation (annihilation) field to a larger positive (negative) value as the direction of the applied field is changed from the easy-axis to the hard-axis was

attributed by Wernsdorfer to the angular dependence of the demagnetization field. To first order, this picture predicts the correct magnitude of the shift, which for our data is 600 Oe and 800 Oe for the nucleation and annihilation fields, respectively. The greater shift of the annihilation field suggests that the actual critical fields depend on the angle of the applied field in a more complex way.

6. Conclusion

In summary, we have presented MFM measurements of arrays of submicron-scale Co dots fabricated by interference lithography. The data indicates that the magnetic response of these structures is dominated by the uniaxial shape anisotropy of the structures and not the crystalline anisotropy of the Co. This leads to the formation of highly ordered remanent states that are characterized by smoothly varying magnetization patterns and a high degree of uniformity across the array. The behavior exhibited by the dots contrasts with previously reported results on similarly sized Co structures, which showed greater local disorder in the remanent domain patterns. We attribute the higher degree of uniformity and symmetry in our structures to differences in the Co microstructure. Specifically, smaller grain sizes and the lack of texturing result in a stronger intergrannular exchange coupling, which mitigates the effects of crystalline anisotropy.

The MFM data are consistent with magnetic hysteresis measurements of the arrays, and both sets of data are in agreement with our micromagnetic simulations. Altogether, the MFM data, the hysteresis loops and the simulations provide a complete picture of the reversal mechanism in these structures. In this size regime,

reversal in each dot is initiated by the nucleation of a single vortex at one end of the dot. As the applied field is reduced, the vortex is swept to the opposite end of the dot where, at a critical field, it is annihilated. The observed nucleation and annihilation fields are modulated by the demagnetization field, which depends on the angle of the applied field. Thus, the only significant distinction between reversal in the easy-axis and reversal the hard-axis is in the field values for nucleation and annihilation. The two different saturation remanent states (i.e. uniform magnetization and single-vortex) represent the two basic configurations that describe the same reversal process.

Acknowledgments

This work was performed at the Lawrence Livermore National Laboratory for the Department of Energy under contract No. W-7405-Eng-48. Assistance from Digital Measurements Systems in taking the hysteresis loops in Fig. 6 is greatly appreciated.

References

[1] C. Miramond, C. Fermon, F. Rousseaux, D. Decanini, and F. Carenac, J. Magn. Magn. Mater. 165 (1997) 500.

[2] R. O'Barr, and S. Schultz, J. Appl. Phys. 81 (1997) 5458.

[3] M. Hehn, K. Ounadjela, J. P. Bucher, F. Rousseaux, D. Decanini, B. Bartenlian, and C. Chappert, Science 272 (1996) 1782.

[4] L. Kong, and S. Y. Chou, J. Appl. Phys. 80 (1996) 5205.

[5] R. M. H. New, R. F. W. Pease, and R. L. White, J. Magn. Magn. Mater. 155 (1996) 140.

[6] A. B. Johnston, J. N. Chapman, B. Khamsehpour, and C. D. W. Wilkinson, J. Phys. D 29 (1996) 1419.

[7] S. McVitie, and J. N. Chapman, IEEE Transactions on Magnetics 24 (1988) 1778.

[8] E. C. Stoner, and E. P. Wohlfarth, Philos. Trans. Soc. London A 240 (1948) 599.

[9] W. Wernsdorfer, K. Hasselbach, A. Benoit, G. Cernicchiaro, D. Mailly, B. Barbara, and L. Thomas, J. Magn. Magn. Mater. 151 (1995) 38.

[10] W. Wernsdorfer, B. Doudin, D. Mailly, K. Hasselbach, A. Benoit, J. Meier, J.-P. Ansermet, and B. Barbara, Phys. Rev. Lett. 77 (1996) 1873.

[11] M. Lederman, D. R. Fredkin, R. O'Barr, S. Schultz, and M. Ozaki, J. Appl. Phys. 75 (1994) 6217.

[12] R. M. H. New, R. F. W. Pease, and R. L. White, J. Vac. Sci. Technol. B 13 (1995) 1089.

[13] A. Fernandez, P. J. Bedrossian, S. L. Baker, S. P. Vernon, and D. R. Kania, IEEE Trans. Magn. 32 (1996) 4472.

[14] A. Fernandez, H. T. Nguyen, J. A. Britten, R. D. Boyd, D. R. Kania, A. M. Hawryluk, and M. D. Perry, J. Vac. Sci. Technol. B 15 (1997) 729.

[15] A. Fernandez, J. Y. Decker, S. M. Herman, D. W. Phillion, D. W. Sweeney, and M. D. Perry, J. Vac. Sci. Technol. B 15 (1997) 2439.

[16] LiftMode is a registered trademark of Digital Instruments. V. Elings, and J. Gurley, U. S. Patent No. 5,308,974, Digital Instruments, Santa Barbara, CA.

[17] M. R. Gibbons, J. Magn. Magn. Mater. , accepted for publication (1998) .

[18] K. Babcock, M. Dugas, S. Manalis, and V. Elings, Mater. Res. Soc. Symp. Proc. 355 (1995) 311.

[19] D. R. Fredkin, and T. R. Koehler, J. Appl. Phys. 67 (1990) 5544.

[20] M. R. Gibbons, A. Fernandez, and C. J. Cerjan, J. Appl. Phys. (1998) submitted for publication.

[21] G. A. Gibson, and S. Shultz, J. Appl. Phys. 73 (1993) 4516.

[22] R. D. Gomez, M. C. Shih, R. M. H. New, R. F. W. Pease, and R. L. White, J. Appl. Phys. 80 (1996) 342.

[23] W. Wernsdorfer, K. Hasselbach, A. Sulpice, A. Benoit, J.-E. Wegrowe, L. Thomas, B. Barbara, and D. Mailly, Phys. Rev. B. 53 (1996) 3341.

Figure Captions

Fig. 1 Scanning electron micrograph of an array of polycrystalline Co dots patterned by interference lithography. The dots in this image measure 430 nm×270 nm.

Fig. 2 (a) Magnetic force image of an array of 180 Å thick Co dots after saturating the dots along their long-axes and then removing the field. The image shows that the dots are uniformly magnetized parallel to the long-axis. (b) A larger scale magnetic force image of the array in (a) illustrating the high degree of uniformity achieved on this sample.

Fig. 3 (a) Magnetic force image of a 180 Å thick Co dot after saturating the sample in the hard-axis direction and then removing the field. The contrast here indicates that the dot has relaxed into a flux closure pattern in which a single vortex occupies the center of the dot. (b) Magnetic force image of an array 180 Å thick Co dots in the hard-axis remanent state. This image shows that both signs of vortex circulation are present.

Fig. 4 Simulation results for the hard-axis remanent state of the polycrystalline Co dots. (a) A simulated MFM image of the hard-axis remanent state, which reproduces the same contrast seen in the experimental data. (b) The corresponding magnetization configuration showing a single-vortex closure pattern. The actual discretization is two times finer than what is displayed.

Fig. 5 Magnetic force image of an array of 300 Å thick dots in a minor-loop remanent state. The dots were first saturated in the easy-axis direction, and then a reverse field of -300 Oe was applied. This image is evidence that the dots reverse their magnetization by the nucleation and annihilation of a single vortex.

Fig. 6 Magnetic hysteresis loops for an array of 300 Å thick Co dots measured with a Digital Measurements Systems vibrating sample magnetometer. The easy-axis loop in (a) shows a large remanence and a coercivity of 155 Oe. The hard-axis loop in (b) shows zero remanence, which is consistent with our interpretation of the MFM data. The transitions labeled H_n and H_a mark the fields at which nucleation and annihilation of a single vortex occurs, respectively.

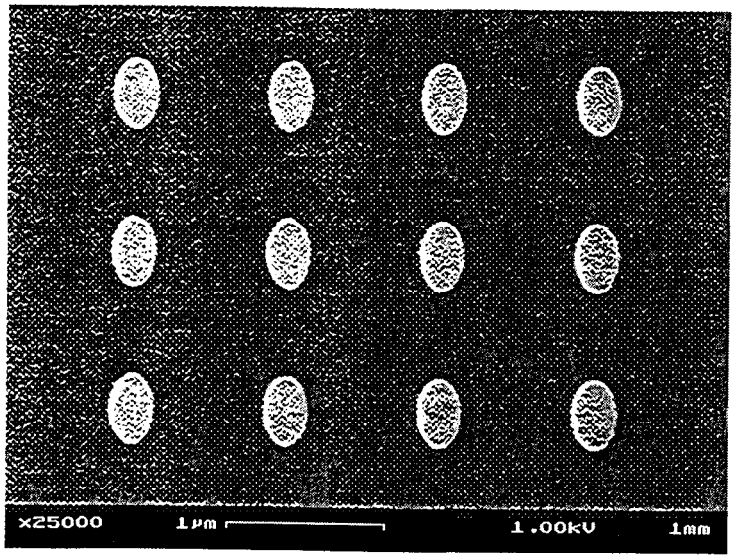

Figure 1

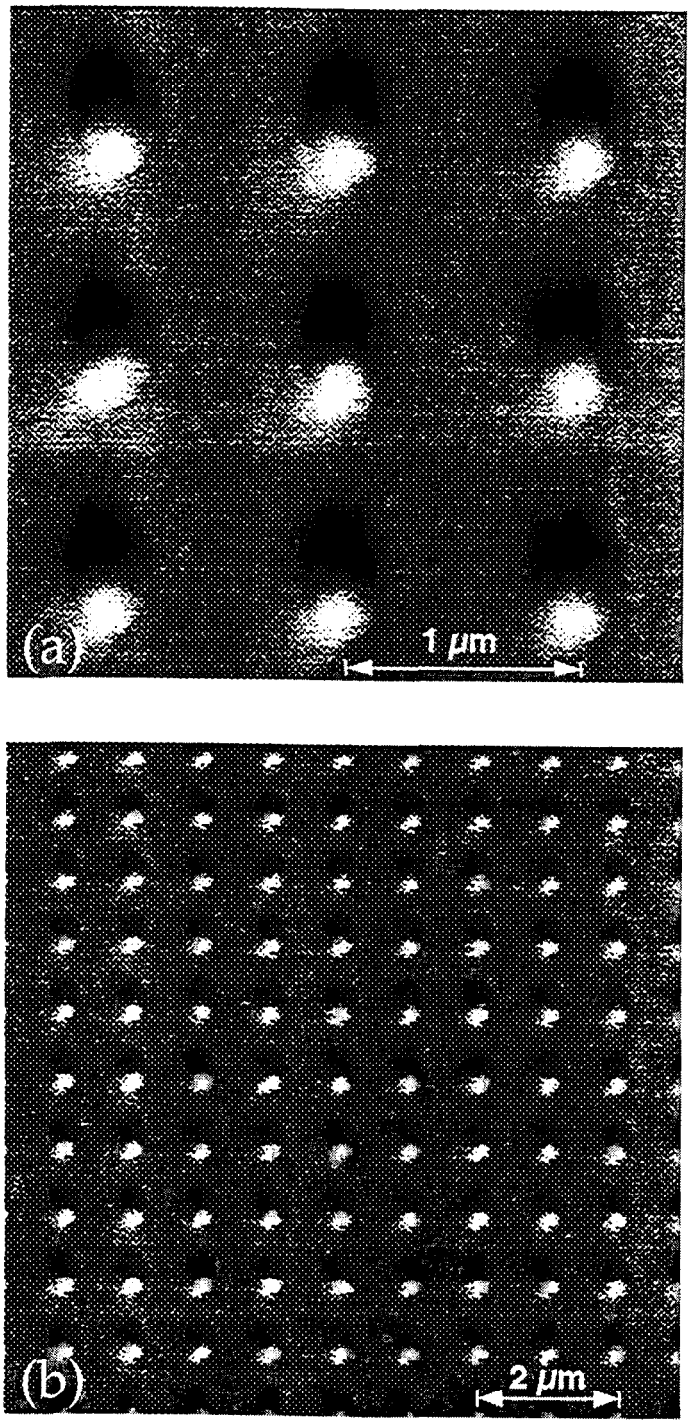

Figure 2

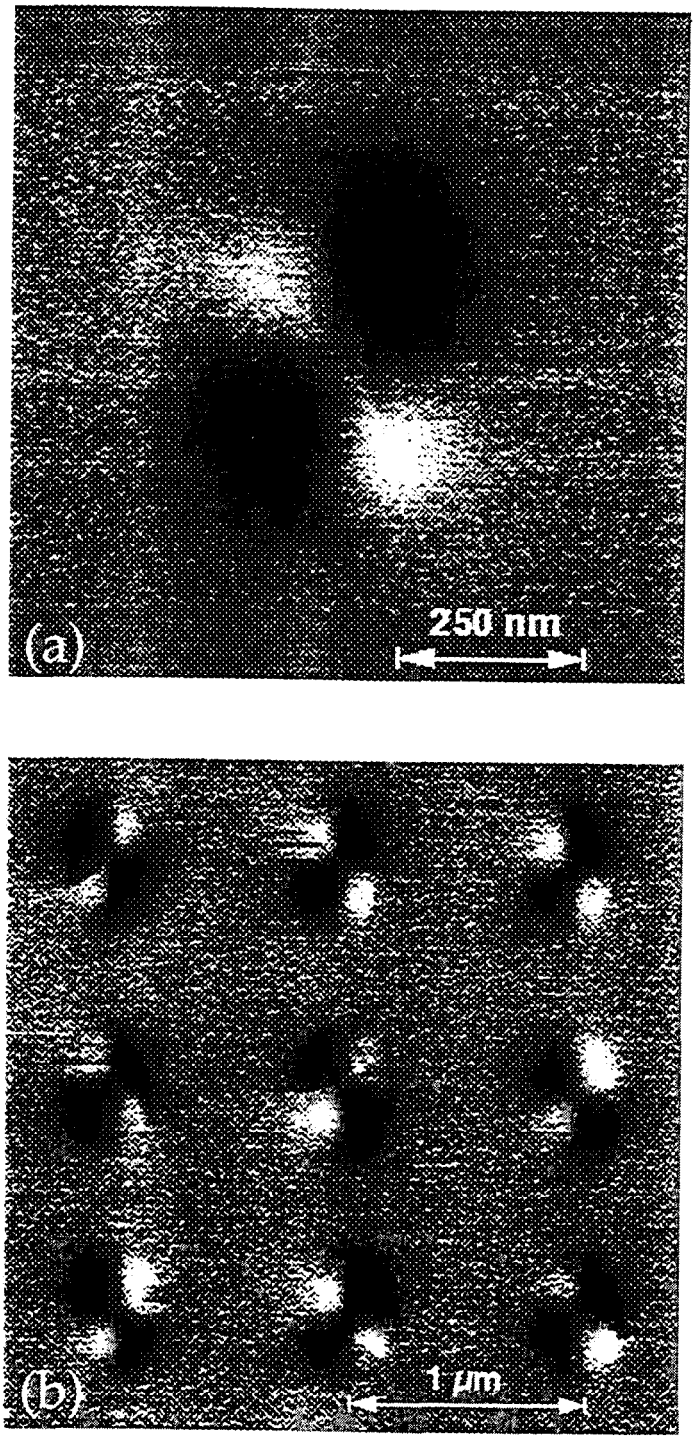

Figure 3

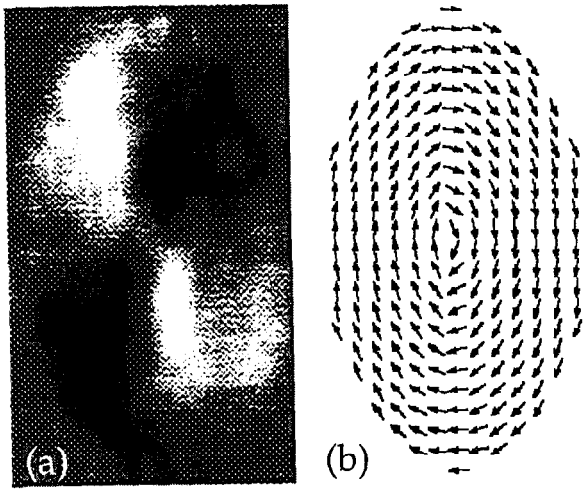

Figure 4

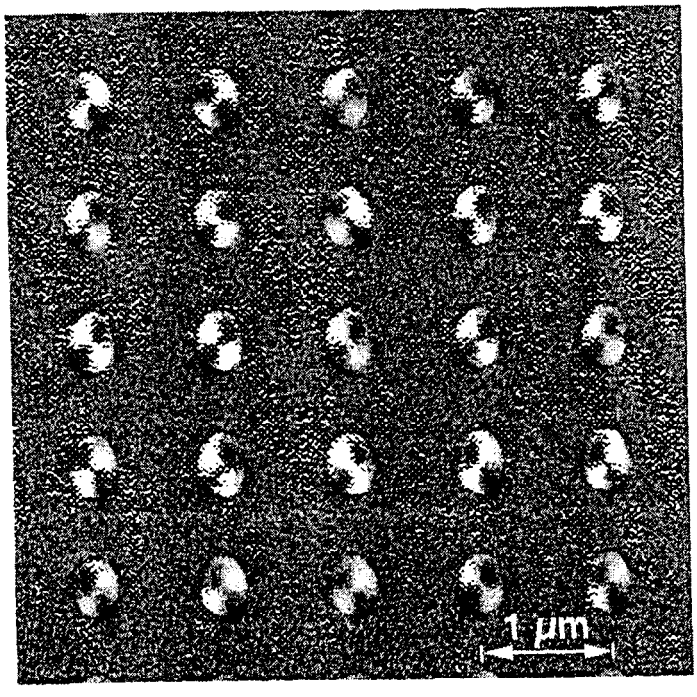

Figure 5

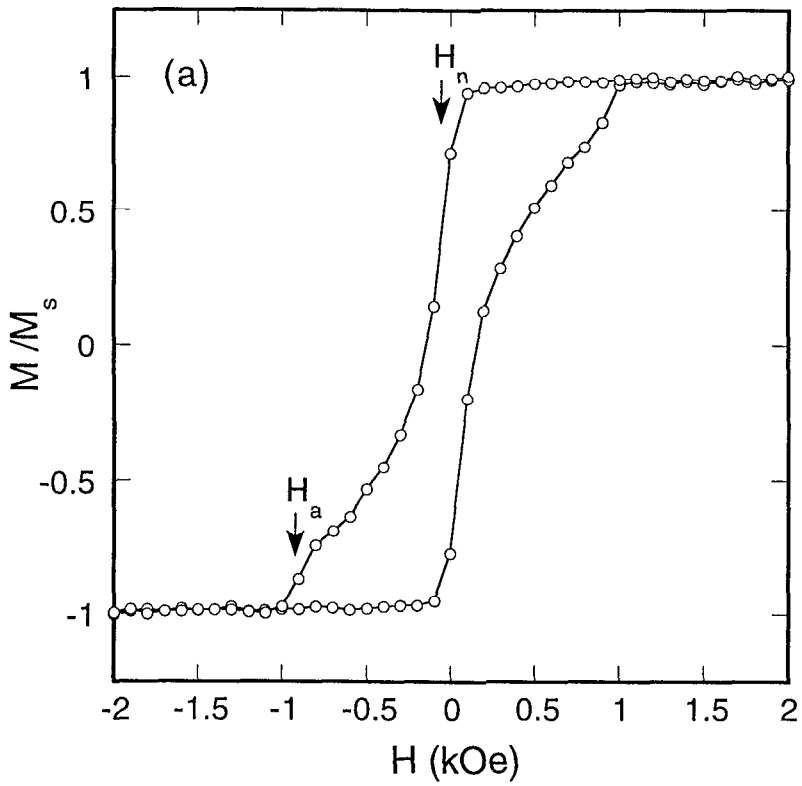
(a)
H_n
H_a
M /M_s
H (kOe)
1
0.5
0
-0.5
-1
-2
-1.5
-1
-0.5
0
0.5
1
1.5
2

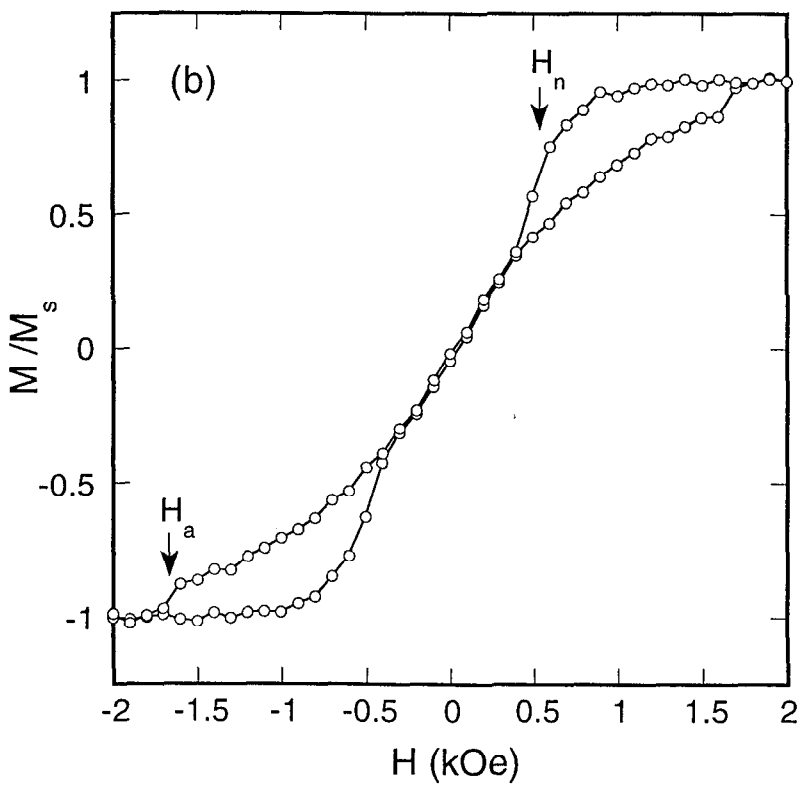
(b)
H_n
H_a
M /M_s
H (kOe)
1
0.5
0
-0.5
-1
-2
-1.5
-1
-0.5
0
0.5
1
1.5
2

Technical Information Department • **Lawrence Livermore National Laboratory**
University of California • Livermore, California 94551